

Endothelium capture-based liver segment imaging using vascular endothelial growth factor receptor 2 in preclinical *ex vivo* models

D. Kyuno^{1,2} , B. Qian¹, W. Groß¹, M. Schäfer¹ and E. Ryschich¹

¹Department of General, Visceral and Transplantation Surgery, University Hospital Heidelberg, Heidelberg, Germany, and ²Department of Surgery, Surgical Oncology and Science, Sapporo Medical University, Sapporo, Japan

Correspondence to: Dr E. Ryschich, Department of General, Visceral and Transplantation Surgery, University Hospital Heidelberg, Im Neuenheimer Feld 365, 69120 Heidelberg, Germany (e-mail: eduard.ryschich@med.uni-heidelberg.de)

Background: Near-infrared (NIR) imaging of liver segments provides substantial information for surgeons performing liver resection. It was hypothesized that ramucirumab, an endothelium-specific antibody approved by the Food and Drug Administration, could be used for liver segment imaging using the endothelium capture principle.

Methods: The capture efficacy of anti-vascular endothelial growth factor receptor (VEGFR) 2 monoclonal antibodies (mAbs) and segment imaging were studied in a mouse model. Binding of ramucirumab in human and porcine tissues was studied using immunofluorescence staining. Isolated porcine liver perfusion was used to analyse the labelling and NIR imaging of selected liver segments.

Results: VEGFR2 is well expressed on the endothelium of the smallest microvascular blood vessels in mouse, porcine and human liver tissues, as well as in human liver tumours. Perfusion of selected segments in the isolated liver model showed high capture of the anti-VEGFR2 (clone 522302) mAb and ramucirumab in mice and pigs respectively. NIR imaging of selected segments was achieved using isolated porcine liver perfusion with IRDye[®] 800CW-conjugated ramucirumab.

Conclusion: VEGFR2 is well expressed on the smallest microvascular blood vessels and can capture antibodies during single intravascular passages with high efficacy. The *ex vivo* imaging of a selected segment using endothelial capture of ramucirumab demonstrates the potential of this antibody for intraoperative navigation in liver surgery.

Surgical relevance

Imaging of liver segments provides substantial information for surgeons when performing liver resection.

The antivascular endothelial growth factor receptor (VEGFR) 2 antibody ramucirumab conjugated with near-infrared dye could visualize selected liver segments using

an endothelial capture-based approach in an isolated perfusion liver model.

The *ex vivo* imaging of a selected segment using endothelial capture of ramucirumab demonstrates the potential of this anti-VEGFR2 antibody for intraoperative navigation in liver surgery.

Funding information

Uehara Memorial Foundation
ITO Foundation for the Promotion of Medical Science
China Scholarship Council, 201506090161

Paper accepted 20 November 2019

Published online 22 January 2020 in Wiley Online Library (www.bjsopen.com). DOI: 10.1002/bjs.5.50253

Introduction

Resection of cancer-bearing areas of the liver is the curative option for the treatment of liver cancer¹ and liver metastasis of gastroenterological tumours², but hepatectomy is

associated with a relatively high risk of complications, such as bleeding, biliary leakage and acute liver failure³. The extent of surgical intervention is crucial for the development of postoperative complications and for the outcome: the larger the resected liver volume, the greater

the morbidity and mortality rates⁴. For this reason, the concept of parenchyma-sparing hepatectomy has been developed^{2,4}. In anatomical hepatectomy, minimal loss of liver tissue can be achieved by resecting a single segment (segmentectomy). Sparing of liver tissue is especially important in patients with reduced liver function, particularly those suffering from chronic hepatitis or cirrhosis⁵.

The identification of liver segments is done during surgery, taking into account the anatomical–functional division according to Couinaud⁶ and Bismuth⁷. As the anatomy of liver segments is highly variable, the individual anatomy of the patient must be identified during the operation⁵. This is achieved by ‘intraoperative navigation’, such as the identification of large blood vessels using intraoperative ultrasound-guided dye injection⁸.

Recently, there has been increasing interest in image-guided surgery using fluorophores for the intraoperative detection of tumours and organs. Optical fluorescence imaging has been developed to visualize the anatomical structure of organs and to monitor biological information of tumours⁹. For optical imaging, the use of near-infrared (NIR) fluorophores offers several advantages. NIR fluorescence imaging within the wavelength range of 700–1000 nm has very low absorption and autofluorescence from the organs, and provides a clear contrast between target and background tissues with high sensitivity and accuracy¹⁰. Indocyanine green (ICG) is the clinically approved NIR dye that is used for intraoperative navigation^{11–13}. ICG fluorescence imaging is advantageous for labelling selected hepatic segments compared with the technique using only indigocarmine¹¹.

As soon as circulating antibodies have been administered systemically, they have direct contact with endothelial cells¹⁴. Thus, endothelium-specific antibodies could bind to specific antigens immediately after application. Currently, one endothelium-specific antibody, ramucirumab, has been approved by the US Food and Drug Administration¹⁵. This antibody binds to vascular endothelial growth factor receptor (VEGFR) 2, and has been approved for the treatment of gastric, oesophageal, colorectal and lung carcinomas¹⁶. Recently, the phenomenon of endothelial capture (endocapt) was described¹⁴. This phenomenon allows almost complete removal of the antibody after its superselective intravascular injection and leads to immediate site-specific antibody enrichment. In the present study, the potential of VEGFR2 and ramucirumab was analysed for use in an endocapt-based approach to image selected liver segments using experimental models.

Methods

Antibodies

Antibodies are listed in *Table S1* (supporting information).

Cell culture

Human dermal microvascular endothelial cells (HDMEC) (PromoCell, Heidelberg, Germany) were used in cell culture experiments. HDMEC were cultured in the endothelial cell medium MV2 (PromoCell) and incubated at 37°C in 5 per cent carbon dioxide.

Immunofluorescence staining

Patients included in the study were admitted to the Department of Surgery, University of Heidelberg. The protocol was approved by the local ethics committee and informed consent was obtained according to the Helsinki Declaration. Tissue samples were snap-frozen and stored in liquid nitrogen. Samples of hepatocellular carcinoma ($n = 5$) and pancreatic cancer liver metastases ($n = 4$) were stained with ramucirumab using two-step immunofluorescence followed by vascular counterstaining with anti-cluster of differentiation (CD) 31 or CD105 monoclonal antibodies (mAbs) (*Tables S1* and *S2*, supporting information).

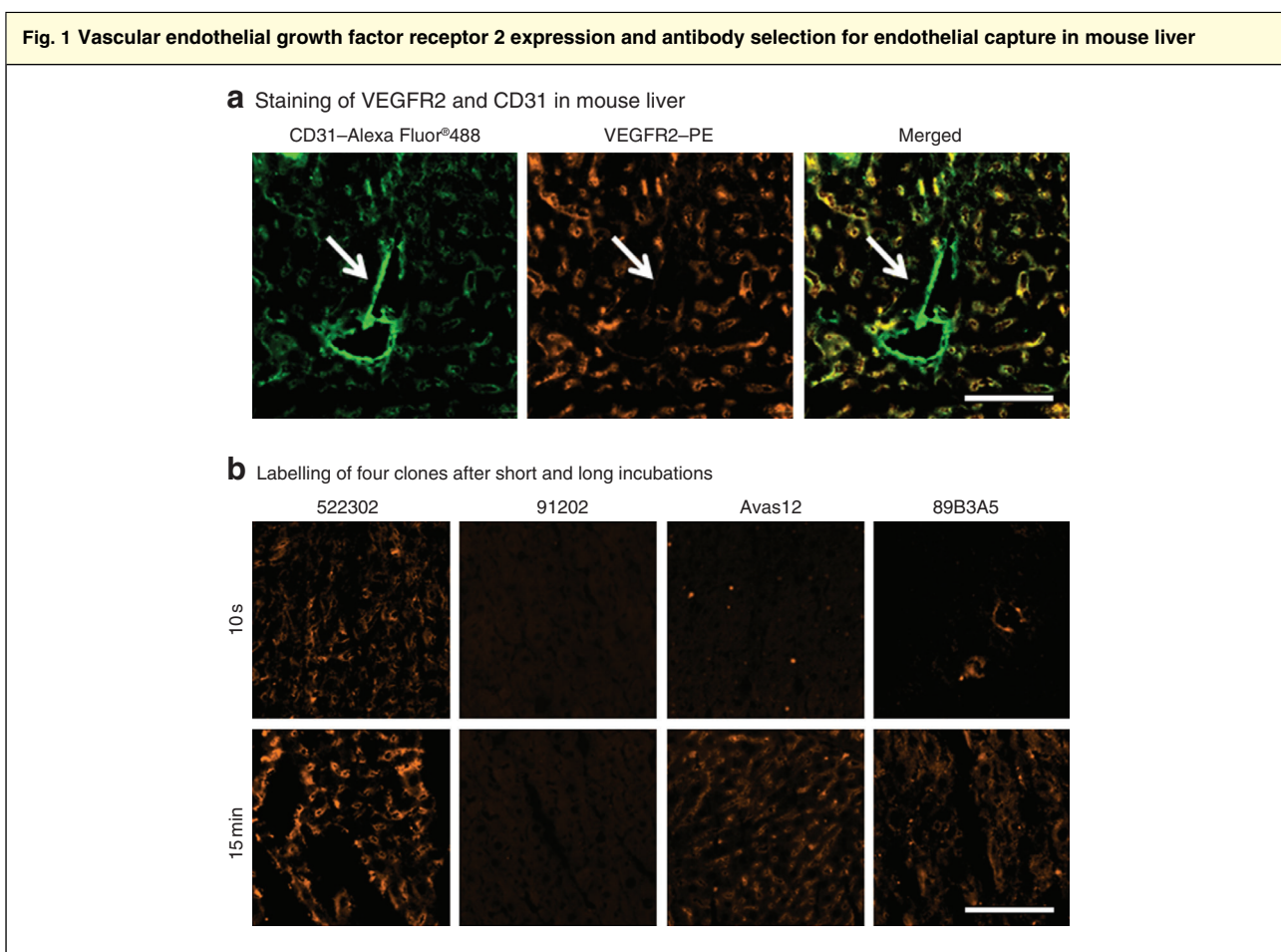
For staining, each slide (7- μ m thick frozen sections) was incubated with antibodies for 30 min at room temperature. After staining, the slides were washed three times with phosphate buffer solution (PBS). The stained tissues were visualized and analysed using fluorescence microscopy (Axio Observer Z1; Zeiss, Jena, Germany). All images were collected and processed using ZEN 2011 software (Zeiss).

For immunofluorescence staining of HDMEC, cells were cultured in a monolayer in μ -Slide VI 0.4 chambers (Ibidi, Martinsried, Germany). The cells were incubated for 30 min at room temperature with 30 μ l of the antibody. The antibody was removed by washing with PBS.

For image-based quantitative analyses to measure the mean fluorescence intensity (MFI), the tissues were incubated with antibodies for 15 min or 10 s. When the purified antibodies (*Table S2*, supporting information) were used, the secondary antibodies (*Table S1*, supporting information) were used at 0.4 μ g/ml for 30 min. Each MFI value was corrected for the background. All experiments were repeated three times.

Fluorescent probes and antibody labelling

IRDye[®] 800CW *N*-hydroxysuccinimide (NHS) ester (IRDye[®] 800CW), IRDye[®] 700DX NHS ester (IRDye[®] 700DX) and IRDye[®] 650 NHS ester (IRDye[®] 650) were used as fluorescent probes (all IRDye[®] probes from



a Immunofluorescence staining of vascular endothelial growth factor receptor (VEGFR) 2 and cluster of differentiation (CD) 31 in mouse liver. Small blood vessels were readily stained by both anti-VEGFR2 (clone 522302) and CD31 (clone 390) monoclonal antibodies, whereas only CD31 was expressed on larger blood vessels (arrows). PE, R-phycoerythrin. **b** Representative images of selected anti-VEGFR2 clones using 15 min and 10 s incubation times. Scale bars, 100 μ m.

LI-COR Biosciences, Lincoln, Nebraska, USA). The above probes have absorption/emission peaks of 778/794, 689/700 and 648/665 nm respectively.

Antibodies including ramucirumab (Table S3, supporting information) were labelled with the fluorescent probes according to the manufacturer's protocol. Unconjugated dye was removed by dialysis (Slide-A-Lyzer™; Thermo Fisher, Waltham, Massachusetts, USA). The calculated molecular ratio of dye per protein was confirmed to be 1 : 1 to 3 : 1.

IRDye® 680RD carboxylate (LI-COR Biosciences) was used as a non-reactive fluorescent dye; it has absorption and emission peaks of 672/694 nm.

Isolated mouse liver perfusion

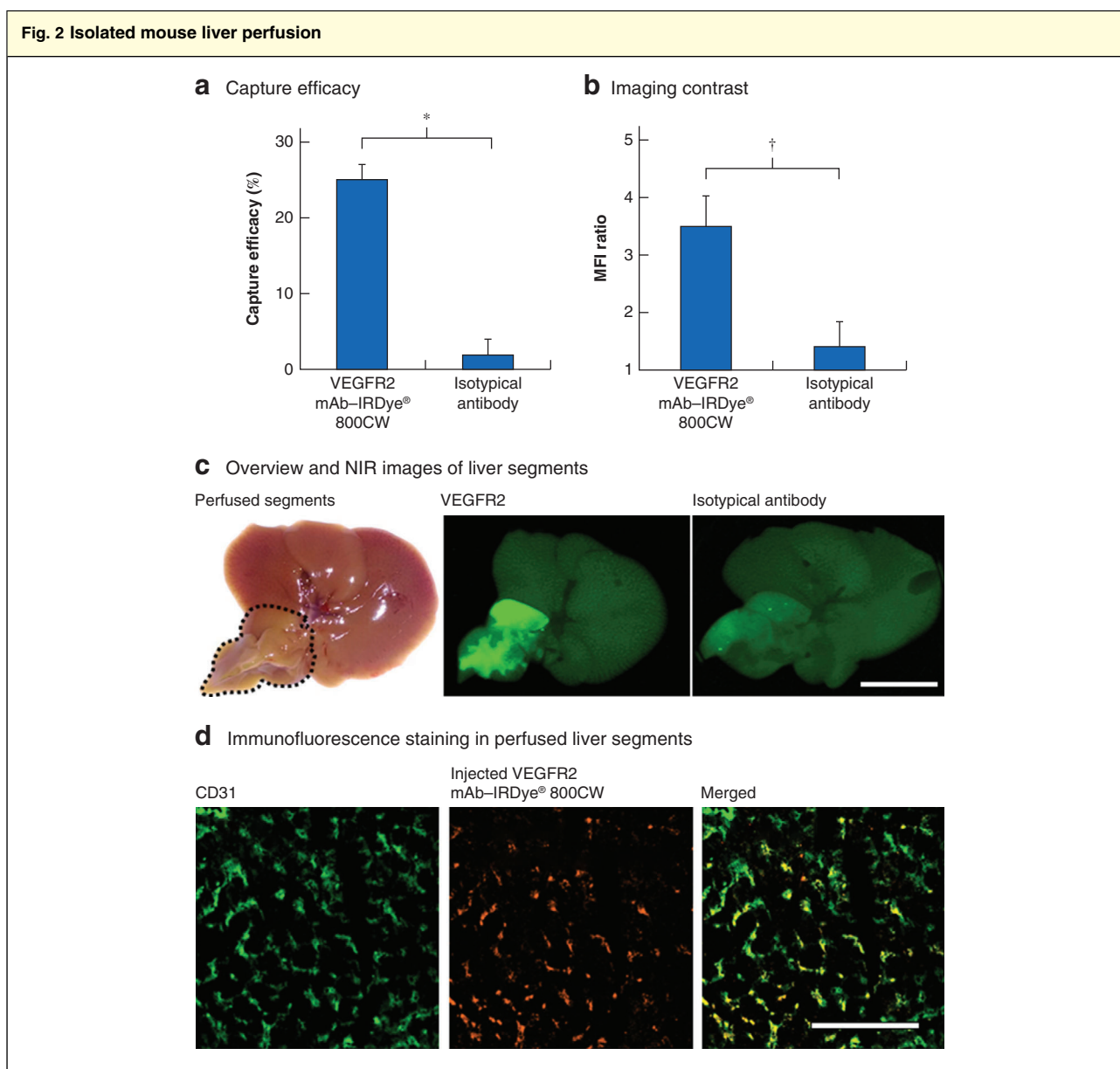
Animals (mice and pigs) were cared for according to national animal welfare regulations and international

recommendations¹⁷. Livers were isolated from animals immediately after they were killed, as described below.

The antimouse VEGFR2 antibody conjugated with IRDye® 800CW and the isotypical antibody were used for the isolated mouse liver perfusion experiments. The livers of five C57BL/6N mice (Charles River, Sulzfeld, Germany) were isolated after the animals were killed with carbon dioxide, and prepared for perfusion as described previously¹⁴. After perfusion, the capture efficacy and the MFI values of the liver were analysed using a NIR imager (Odyssey® CLx; LI-COR Biosciences).

Isolated porcine liver perfusion

Five male domestic pigs (20–25 kg) (Bräunling, Nussloch, Germany) were used for the study. Under sedative medication using azaperone 8 mg/kg (Elanco, Bad Homburg,



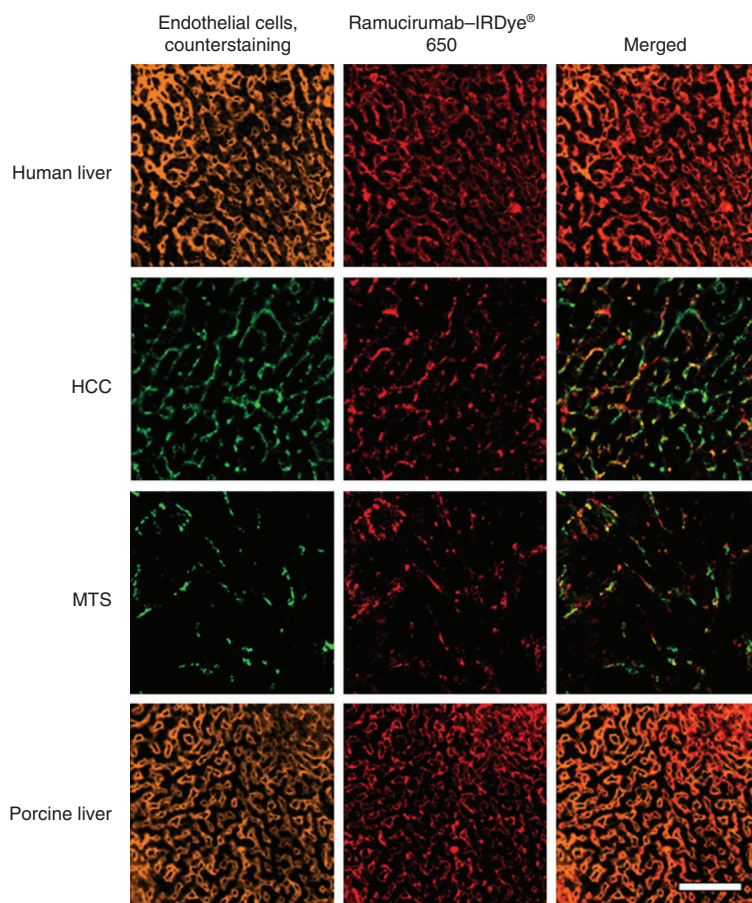
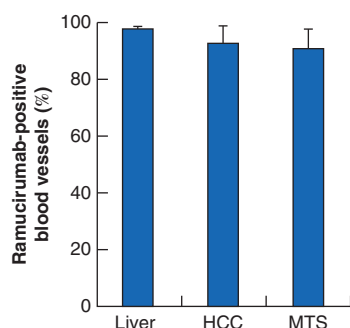
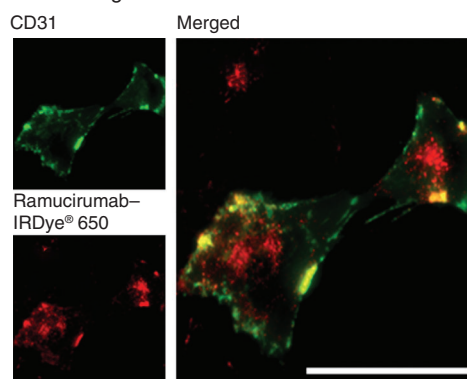
a Capture efficacy of IRDye[®] 800CW-labelled anti-vascular endothelial growth factor receptor (VEGFR) 2 monoclonal antibody (mAb). **b** Imaging contrast calculated as the mean fluorescence intensity (MFI) ratio between perfused and non-perfused liver. **c** Representative overview and near-infrared (NIR) images of liver segments perfused with VEGFR2 or isotypical IRDye[®] 800CW antibodies. Scale bar, 1 cm. **d** Immunofluorescence staining of VEGFR2-IRDye[®] 800CW mAb in perfused liver segments with anti-cluster of differentiation (CD) 31 counterstaining. The bound VEGFR2 antibody was detected by secondary antibody conjugated with R-phycoerythrin. Scale bar, 100 μ m. * $P < 0.001$, † $P = 0.002$ (Student's *t* test).

Germany), midazolam 500 μ g/kg (Hameln Pharma Plus, Hameln, Germany) and ketamine 12–15 mg/kg (Bremer Pharma, Warburg, Germany), the pigs were killed using an intravenous injection of potassium chloride 2 mmol/kg (B. Braun, Melsungen, Germany).

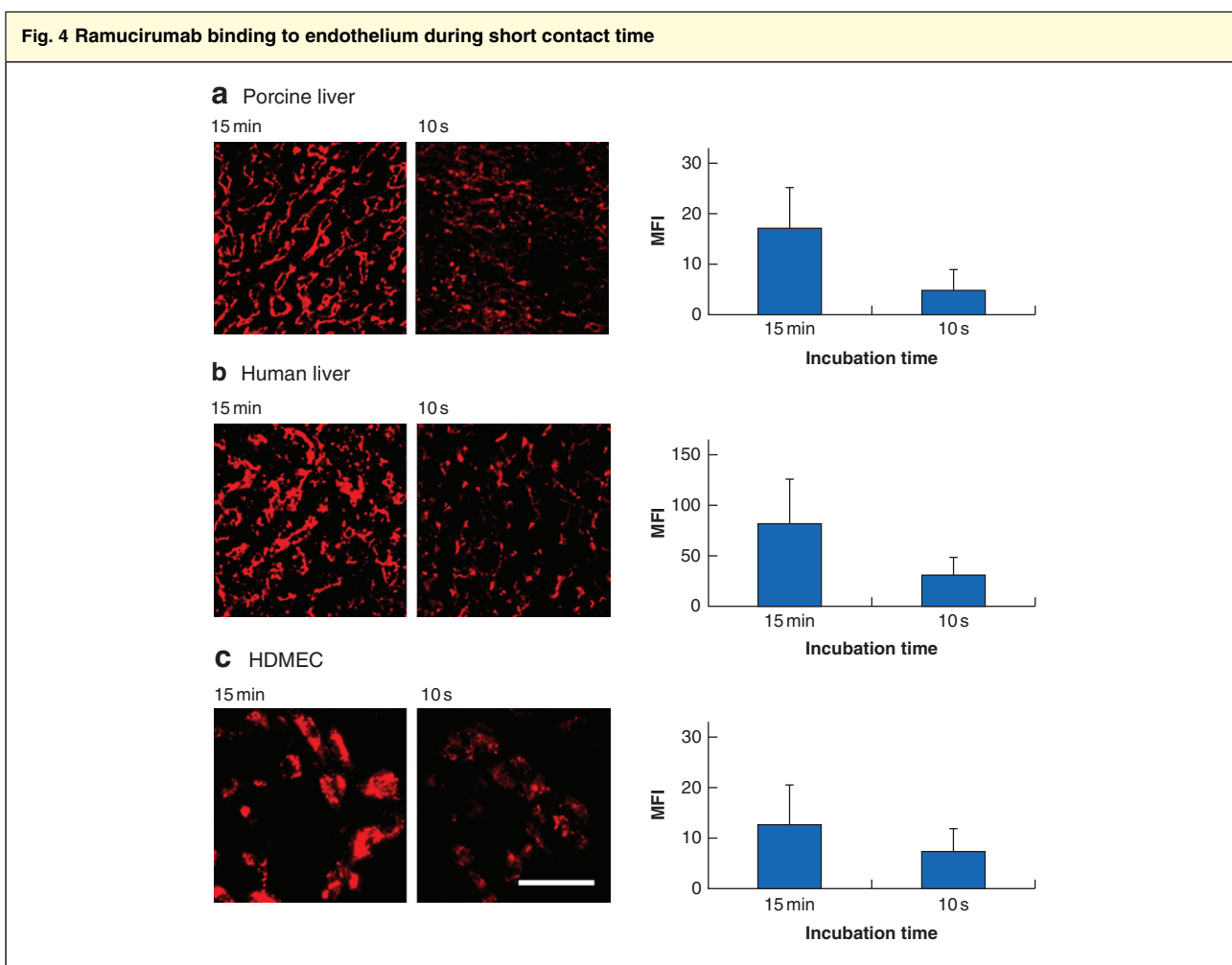
Following midline laparotomy, the portal vein and common hepatic artery were divided after clamping. The liver

was isolated and transferred back to the table immediately. The tube (7 mm in diameter) and 7-Fr catheter (Smiths Medical, Minneapolis, Minnesota, USA) were inserted into the portal vein and hepatic artery respectively.

To evaluate whether ramucirumab could be captured by the endothelium in the liver during intravascular passage, a perfusion system was developed for the isolated

Fig. 3 Binding of ramucirumab in tissues and in the endothelial cell line**a** Staining with IRDye® 650-conjugated ramucirumab**b** Ramucirumab-positive vessels**c** Staining of HDMEC

a Representative images of immunofluorescence staining with IRDye® 650-conjugated ramucirumab. Endothelial cells were counterstained with R-phycoerythrin (PE)-conjugated anti-cluster of differentiation (CD) 105 antibody (human liver), Alexa Fluor® 488-conjugated anti-CD31 antibody (hepatocellular carcinoma (HCC) and liver metastasis (MTS)), and PE-conjugated anti-CD31 antibody (porcine liver). Ramucirumab bound well to the endothelium in all presented tissue types. **b** Counting of ramucirumab-positive blood vessels. The total fraction of ramucirumab-positive blood vessels was greater than 90 per cent. **c** Ramucirumab/CD31 staining of vital human dermal microvascular endothelial cells (HDMEC). Scale bars, 100 µm.



Immunofluorescence staining with ramucirumab in **a** porcine liver, **b** human liver and **c** human dermal microvascular endothelial cells (HDMEC) after 15 min and 10 s of incubation. The fluorescence signal of bound ramucirumab was detected even with 10 s of incubation. MFI, mean fluorescence intensity. Scale bar, 100 μ m.

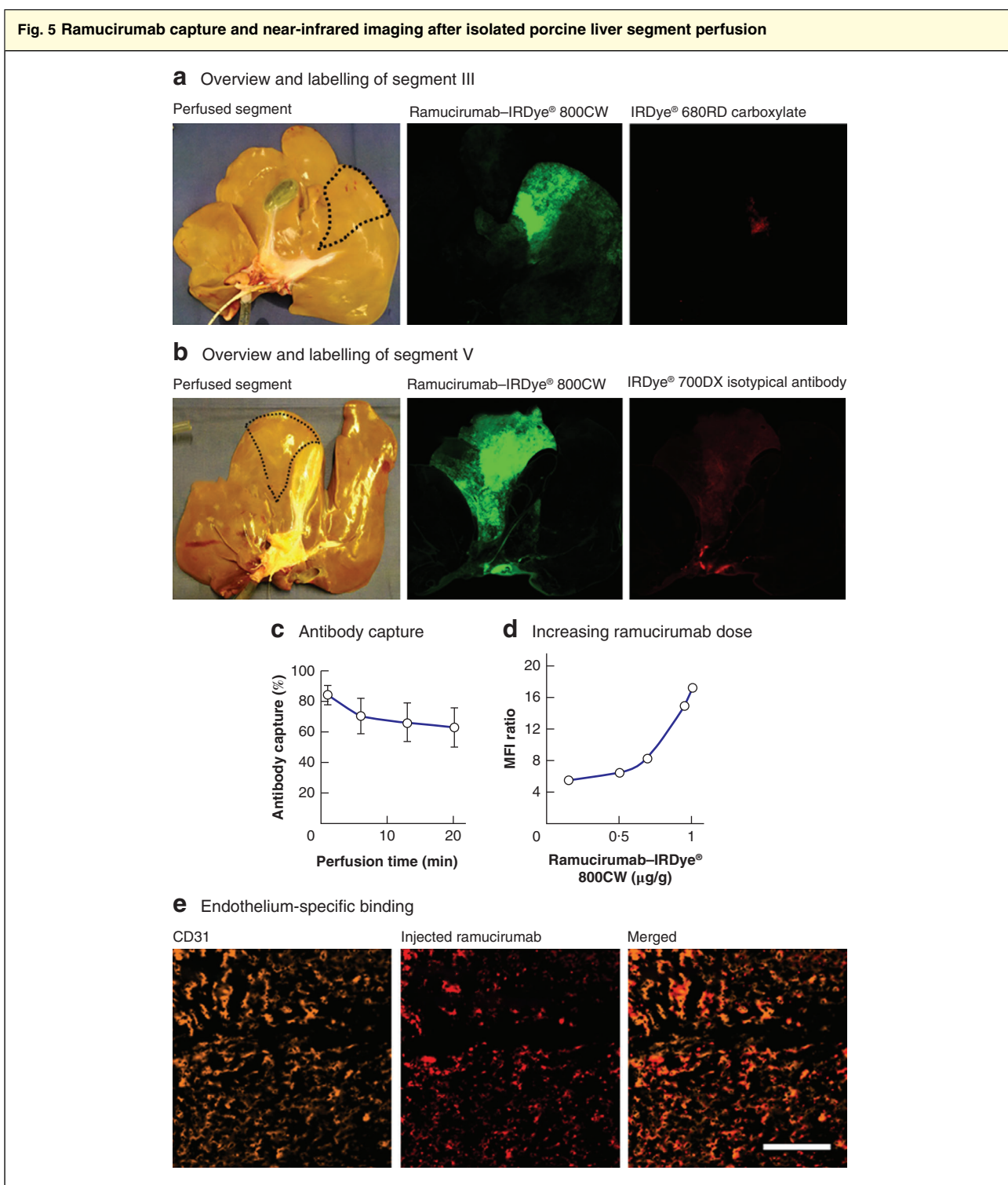
porcine liver (Fig. S1, supporting information). The pressure of the oxygenated Krebs–Henseleit (KH)¹⁸ (5 per cent carbon dioxide and 95 per cent oxygen at 37°C) was controlled at 10 mmHg for the portal vein and 80 mmHg for the hepatic artery. After removal of the blood from the vascular system using perfusion of 1000 ml buffer, a small catheter (0.61 mm) was inserted into the selected segmental artery. The conjugated antibodies were injected, and oxygenated KH buffer was perfused for 20 min. After perfusion, the liver was scanned using the NIR imager, and the MFI values of perfused and unperfused segments were calculated. The MFI value of the perfused segment with ramucirumab conjugated with IRDye® 800CW (ramucirumab–IRDye® 800CW) was normalized by subtracting that of the IRDye® 680RD carboxylate, because residual IRDye® 680RD carboxylate

was regarded as the retention of the dye in the washed liver.

After washing out the liver with the buffer, the amount of unbound antibody was calculated, using a centrifugal concentrator, Vivaspin® (Sartorius Lab Instruments, Göttingen, Germany), because a concentration lower than 100 ng/ml could not be measured correctly in a large volume of the fluid.

Statistical analysis

Statistical analysis was performed with SPSS® version 21 (IBM, Armonk, New York, USA). Data are shown as the mean(s.d.) values. To study differences between the groups, Student's *t* test was used. $P < 0.050$ was considered statistically significant.



a,b Labelling after selective perfusion of liver segments III (**a**) and V (**b**). IRDye® 800CW-conjugated ramucirumab was captured effectively in the liver segment, attaining strong near-infrared imaging contrast. Control substances (IRDye® 680RD carboxylate (**a**) and isotypical antibody (**b**)) were removed almost completely. **c** Quantitative analysis of antibody capture after perfusion of porcine liver. **d** Step-by-step increase in ramucirumab dose up to 1 µg/g tissue resulted in increasing fluorescence contrast. **e** Representative images of immunofluorescence staining confirmed the endothelium-specific binding of ramucirumab in the perfused liver segment. Scale bar, 100 µm.

Results

Endothelial capture of anti-VEGFR2 antibody in isolated mouse liver perfusion

To investigate the expression of VEGFR2 and binding of the antibody to endothelium in the liver, immunofluorescence staining in mouse liver tissue was used. Anti-CD31 mAb was used for the counterstaining of endothelial cells.

VEGFR2 was detected widely in the mouse liver, and showed cellular overlap with the expression of CD31 in the smallest blood vessels. Large blood vessels expressed CD31 but were not stained with anti-VEGFR2 (Fig. 1a). To identify antibody candidates for endocapt, the binding ability after a short incubation time of four different anti-VEGFR2 antibody clones was analysed. Only one of the four antibodies (clone 522302) showed detectable labelling after a short incubation (2 µg/ml for 10 s) (Fig. 1b). This antibody was selected for further experiments.

Capture of IRDye® 800CW-conjugated anti-VEGFR2 (522302) mAb or isotypical antibody was analysed using perfusion of isolated liver segments. The antibody was perfused at a dose of 50 ng per segment, corresponding to approximately 0.1 µg/g tissue. These experiments showed that 522302 mAb was captured with a mean(s.d.) efficacy of 25.0(2.0) per cent by hepatic endothelial cells during the single intravascular passage, whereas capture of the isotypical antibody was low (Fig. 2a). Endothelial capture resulted in a significant accumulation of the fluorescence signal (Fig. 2b) and in high contrast of the perfused liver segments using NIR imaging (Fig. 2c). The capture of anti-VEGFR2 mAb by endothelial cells was confirmed histologically by fluorescence staining with the secondary antibody on histological slides and counterstaining of CD31 (Fig. 2d).

Ramucirumab labelling of endothelium of porcine and human normal livers and hepatic tumours

Immunofluorescence staining showed that ramucirumab was specifically bound in human and porcine normal liver tissue and in human hepatocellular carcinoma and metastases of pancreatic cancer (Fig. 3a). As shown by counterstaining of blood vessels with anti-CD105 or anti-CD31 antibodies, almost all capillaries and sinusoidal microvessels bound ramucirumab, whereas larger blood vessels were ramucirumab-negative (Fig. S2, supporting information). The total fraction of ramucirumab-positive blood vessels was above 90 per cent (Fig. 3b). Ramucirumab also bound to vital endothelial cells, demonstrating the extracellular localization of the binding epitope (Fig. 3c).

Ramucirumab binding and imaging in isolated porcine liver perfusion

To study the potential of ramucirumab for endocapt application, its binding ability after a short incubation time in histological slides or in vital endothelial cells was analysed. It was found that both human and porcine liver endothelium, as well as vital HDMEC, showed a readily detectable fluorescence signal after a 10-s incubation of unlabelled ramucirumab using two-step immunofluorescence (Fig. 4).

In addition, the endocapt procedure was analysed using perfusion of the porcine liver segment *ex vivo*. IRDye® 800CW-conjugated ramucirumab was captured effectively in the perfused liver segment (mean(s.d.) 62.6(13.0) per cent) (Fig. 5c) and was contrasted using NIR imaging (Fig. 5a,b). The step-by-step increase in the ramucirumab dose up to 1 µg/g tissue resulted in the respective increase of fluorescence contrast (Fig. 5d). In contrast to ramucirumab, both the control substance for fluorescence (IRDye® 680RD carboxylate) (Fig. 5a) and IRDye® 700CW-labelled isotypical mAb (Fig. 5b) were almost completely removed by perfusion. Histological studies confirmed specific ramucirumab binding to the endothelium of the perfused liver segment (Fig. 5e).

Discussion

In this study, expression of VEGFR2 and the binding of different antibody clones to this receptor were analysed using liver tissues from different species. VEGFR2 expression was localized on endothelial cells of the smallest blood vessels, and was identical in mice, pigs and humans. As shown previously¹⁴, effective epitope binding within a very short time is an important prerequisite of endothelium-specific antibodies as candidates for endocapt. This characteristic can be verified by the detection of antibody binding after incubation of 10 s and/or by the calculation of half-effective antibody concentration of binding on histological slides¹⁴. As expected, the binding speed of different antibody clones to VEGFR2 was different in mouse tissue. One of four clones (522302) showed detectable binding in histological slides after 10 s of incubation, and represented clear visualization of the perfused liver segments.

Interestingly, the human anti-VEGFR2 antibody, ramucirumab, demonstrated good cross-reactivity with porcine liver endothelium. This is a favourable situation because it allows endothelial capture of human antibodies to be studied in a porcine model. In the isolated porcine liver, ramucirumab-IRDye® 800CW was captured with high efficacy (above 60 per cent). This facilitated excellent NIR imaging of selected porcine segments. Provided that the binding of ramucirumab in humans is at least as good

as that in pigs, ramucirumab could have a high potential for endocapt-based approaches in humans. Several promising endothelial antigens, such as CD31, CD34 and CD49e, have been proposed previously for use in human endocapt-based approaches^{14,19}. It has also been shown¹⁴ that the capture efficacy of selected antibodies can theoretically achieve a high level of above 90 per cent. Unfortunately, direct comparison of ramucirumab and other antibody clones in the preclinical (porcine) model is not feasible because ramucirumab is the only antibody that cross-reacts with porcine endothelium.

Results of the present study provide a rationale for the use of the anti-VEGFR2 antibody to image specific liver segments. Potential clinical implications for this include fluorescence-guided navigation during parenchyma-sparing liver resection. This operation is highly demanding and aims to save as much normal liver tissue as possible, and to improve the clinical outcome^{2,5}. Parenchyma-sparing liver resection is used mainly in liver tumour surgery and requires exact determination of liver segment anatomy using ultrasonography and/or imaging navigation⁸. Currently, superselective injection of ICG is used for image-guided navigation during liver resection¹¹. Although the use of ICG is a cheap and effective method, there are several potential advantages of endocapt to be considered as a promising alternative. A large fraction of injected ICG is distributed in the systemic circulation, resulting in a continuous reduction of fluorescence contrast between the selected segment and the background¹³. The present authors expect that this negative effect may largely be avoided with the endocapt procedure. Furthermore, ramucirumab had high capture efficacy by the liver endothelium during the single intravascular passage, and may theoretically result in better liver segment demarcation than ICG. The use of endocapt may provide better intraoperative navigation than ICG, helping surgeons to operate more safely and improving the surgical outcome. This hypothesis can be validated only by conducting further *in vivo* and clinical studies.

In the present study, IRDye[®] 800CW was used for antibody labelling and NIR imaging. As shown in rats and non-human primates^{20,21}, IRDye[®] 800CW is non-toxic and currently used for antibody labelling in clinical studies^{22,23}. IRDye[®] 800CW can be proposed as an alternative for ICG when ICG use is not feasible. Its use may be relevant in several clinical situations, such as in patients with an iodine allergy, despite the low number of such patients²⁴.

VEGFR2 labelling is a promising tool for endocapt-based strategies. The present study provides basic information about the use of ramucirumab for imaging of liver

segments in a preclinical model. The high capture of ramucirumab by liver endothelium may be useful for NIR imaging of the selected liver segment, and can be proposed for application in fluorescence-guided navigation in liver surgery. Information regarding the stability of ramucirumab binding, time course of fluorescence background, translational simplicity and effectiveness of this method must be gained from *in vivo* studies.

Acknowledgements

The authors thank S. Bauer for excellent technical assistance.

This study was supported by grants from the Uehara Memorial Foundation, the ITO Foundation for the Promotion of Medical Science (to D.K.) and the China Scholarship Council (to B.Q.).

Disclosure: The authors declare no conflict of interest.

References

- 1 Cauchy F, Soubrane O, Belghiti J. Liver resection for HCC: patient's selection and controversial scenarios. *Best Pract Res Clin Gastroenterol* 2014; **28**: 881–896.
- 2 Mise Y, Aloia TA, Brudvik KW, Schwarz L, Vauthey JN, Conrad C. Parenchymal-sparing hepatectomy in colorectal liver metastasis improves salvageability and survival. *Ann Surg* 2016; **263**: 146–152.
- 3 Midorikawa Y, Kubota K, Takayama T, Toyoda H, Ijichi M, Torzilli G *et al.* A comparative study of postoperative complications after hepatectomy in patients with and without chronic liver disease. *Surgery* 1999; **126**: 484–491.
- 4 Moris D, Dimitroulis D, Vernadakis S, Papalampros A, Spartalis E, Petrou A *et al.* Parenchymal-sparing hepatectomy as the new doctrine in the treatment of liver-metastatic colorectal disease: beyond oncological outcomes. *Anticancer Res* 2017; **37**: 9–14.
- 5 Yoshida H, Katayose Y, Rikiyama T, Motoi F, Onogawa T, Egawa S, *et al.* Segmentectomy of the liver. *J Hepatobiliary Pancreat Sci* 2012; **19**: 67–71.
- 6 Couinaud C. Liver anatomy: portal (and suprahepatic) or biliary segmentation. *Dig Surg* 1999; **16**: 459–467.
- 7 Bismuth H. Surgical anatomy and anatomical surgery of the liver. *World J Surg* 1982; **6**: 3–9.
- 8 Makuuchi M, Hasegawa H, Yamazaki S. Ultrasonically guided subsegmentectomy. *Surg Gynecol Obstet* 1985; **161**: 346–350.
- 9 Virostko J, Xie J, Hallahan DE, Arteaga CL, Gore JC, Manning HC. A molecular imaging paradigm to rapidly profile response to angiogenesis-directed therapy in small animals. *Mol Imaging Biol* 2009; **11**: 204–212.
- 10 Luo S, Zhang E, Su Y, Cheng T, Shi C. A review of NIR dyes in cancer targeting and imaging. *Biomaterials* 2011; **32**: 7127–7138.

- 11 Miyata A, Ishizawa T, Tani K, Shimizu A, Kaneko J, Aoki T *et al.* Reappraisal of a dye-staining technique for anatomic hepatectomy by the concomitant use of indocyanine green fluorescence imaging. *J Am Coll Surg* 2015; **221**: e27–e36.
- 12 Ishizawa T, Zuker NB, Kokudo N, Gayet B. Positive and negative staining of hepatic segments by use of fluorescent imaging techniques during laparoscopic hepatectomy. *Arch Surg* 2012; **147**: 393–394.
- 13 Aoki T, Murakami M, Yasuda D, Shimizu Y, Kusano T, Matsuda K *et al.* Intraoperative fluorescent imaging using indocyanine green for liver mapping and cholangiography. *J Hepatobiliary Pancreat Sci* 2010; **17**: 590–594.
- 14 Winkler N, Strübing F, Groß W, Mier W, Ryschich E. Phenomenon of endothelial antibody capture: principles and potential for locoregional targeting of hepatic tumors. *Hepatology* 2018; **68**: 1804–1816.
- 15 Poole RM, Vaidya A. Ramucirumab: first global approval. *Drugs* 2014; **74**: 1047–1058.
- 16 Vennepureddy A, Singh P, Rastogi R, Atallah JP, Terjanian T. Evolution of ramucirumab in the treatment of cancer – a review of literature. *J Oncol Pharm Pract* 2017; **23**: 525–539.
- 17 Guillen J. FELASA guidelines and recommendations. *J Am Assoc Lab Anim Sci* 2012; **51**: 311–321.
- 18 Bessems M, Doorschodt BM, Dinant S, de Graaf W, van Gulik TM. Machine perfusion preservation of the pig liver using a new preservation solution, polysol. *Transplant Proc* 2006; **38**: 1238–1242.
- 19 Wang Z, Winkler N, Qian B, Groß W, Mehrabi A, Ryschich E. Endothelial capture using antibodies and nanoparticles in human tissues: antigen identification and liver segment imaging. *Acta Biomater* 2019; **97**: 474–489.
- 20 Marshall MV, Draney D, Sevick-Muraca EM, Olive DM. Single-dose intravenous toxicity study of IRDye 800CW in Sprague-Dawley rats. *Mol Imaging Biol* 2010; **12**: 583–594.
- 21 Zinn KR, Korb M, Samuel S, Warram JM, Dion D, Killingsworth C *et al.* IND-directed safety and biodistribution study of intravenously injected cetuximab–IRDye800 in cynomolgus macaques. *Mol Imaging Biol* 2015; **17**: 49–57.
- 22 de Boer E, Warram JM, Tucker MD, Hartman YE, Moore LS, de Jong JS *et al.* *In vivo* fluorescence immunohistochemistry: localization of fluorescently labeled cetuximab in squamous cell carcinomas. *Sci Rep* 2015; **5**: 10169.
- 23 Rosenthal EL, Warram JM, de Boer E, Chung TK, Korb ML, Brandwein-Gensler M *et al.* Safety and tumor specificity of cetuximab–IRDye800 for surgical navigation in head and neck cancer. *Clin Cancer Res* 2015; **21**: 3658–3666.
- 24 Hope-Ross M, Yannuzzi LA, Gragoudas ES, Guyer DR, Slakter JS, Sorenson JA *et al.* Adverse reactions due to indocyanine green. *Ophthalmology* 1994; **101**: 529–533.

Supporting information

Additional supporting information can be found online in the Supporting Information section at the end of the article.